Chapter

Waste Heat Recovery from Fossil-Fired Power Plants by Organic Rankine Cycles

Qiang Liu

Abstract

More than 60% of the world's electricity is still produced from fossil-fired power plants. Recovering heat from flue gas, drained water, and exhaust steam which are discharged in power plants by organic Rankine cycles (ORCs) to generate power is an efficient approach to reduce fossil fuel consumption and greenhouse gas emissions. This chapter proposes conceptual ORC systems for heat recovery of drain from continuous blowdown systems, exhaust flue gas from boilers, and exhaust steam from turbines. The waste heat source temperatures range from 30 to 200°C. Environmentally friendly and nonflammable working fluids including R134a, R1234ze, R236ea, R245fa, R1233zd, and R123 were selected as the working fluids. The parameters of ORC systems were optimized, and the thermodynamic performance was analyzed. The suitable ORC layouts for various kinds of heat sources including drained water, flue gas, and steam were discussed with selecting the proper working fluids. The gross power output of a coal-fired power plant can be increased up to 0.4% by an ORC using the waste heat from the boiler flue gas. The ORCs using turbine exhaust steam with the cooling water as low as 5°C can generate 2–3% more power for a power unit.

Keywords: coal-fired power plant, waste heat recovery, organic Rankine cycle, parametric optimization, working fluid, thermodynamic analysis

1. Introduction

In 2018, the total world electricity generation reached 26,672 TWh [1]. About 64.15% of the total world electricity generation is still from fossil fuels (coal, natural gas, and oil) [1], especially in China, the USA, Japan, Russia, and India. China accounted for 26.2% of the world electricity generation [2]. The installed fossil-fired power capacity is now increased to 1143.67 GW in China which accounts for about 60% of the total installed power capacity; however, 70.4% of electricity was generated from fossil fuels [2]. Now, China is also the world's greatest emitter of greenhouse gases from the burning of fossil fuels.

The development of large-capacity and high-temperature ultra-supercritical fossil-fired power unit is the trend in the world. However, a large number of waste heat are discharge in a power plant. **Figure 1** shows waste heat sources in a typical coal-fired power unit. Therefore, recovering the waste heat is a main approach to

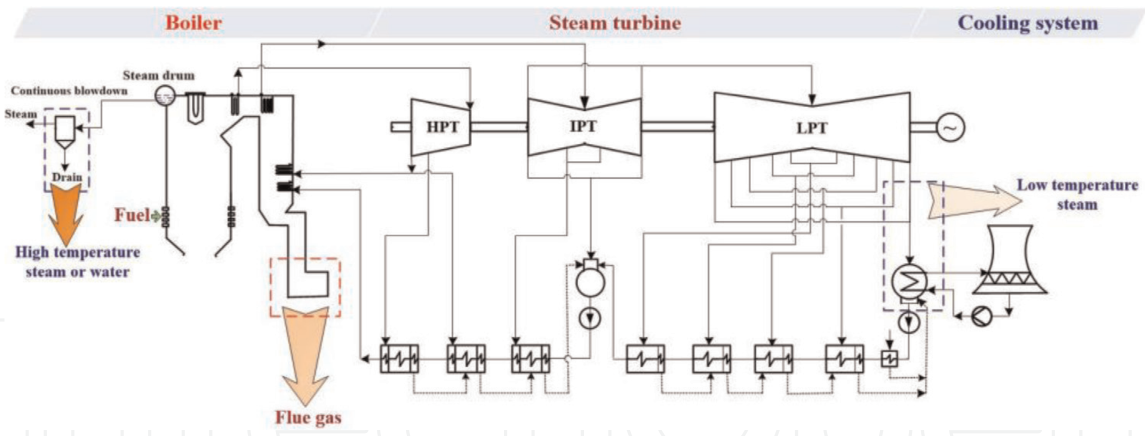

Figure 1.
Schematic of the waste heat sources can be recovered by ORCs in a typical coal-fired power unit.

further improve thermal efficiencies and reduce greenhouse gas emissions for fossil-fired power plants [3].

Continuous blowdown systems are used to purify the steam by removing suspended solids in drum boilers for subcritical power plants as shown in **Figure 1**. A part of the boiler water with temperatures up to 360°C from the drum is discharge to the flash tank. In the flash tank, some of the water flashes to the steam, and then the steam enters into a deaerator or a feedwater heater for feedwater preheating, while the drain is generally discharge to the sewer. The drain temperature is higher than 150°C; however, the heat in the drained water is lost through direct discharge. The waste heat in the drained water can be recovered by an organic Rankine cycle to generate electric power [4].

A modern power station boiler produces large quantities of flue gas. The exhaust flue gas temperatures generally range from 120–140°C for power station boilers. Heat loss due to the exhaust flue gas is the largest heat loss in a power station boiler which significantly affects the boiler thermal efficiency. For large- and medium-capacity boilers, the exhaust flue gas heat loss accounts for 4–8% of the total boiler heat input from fossil burning [3]. In actual operation, the flue gas temperature may be higher than the design value which results in a lower boiler thermal efficiency and a higher fuel consumption. The heat in the exhaust flue gas can be used to preheat feedwater by a low-pressure economizer [5–7] and pre-dry brown coal [8–11]. The waste heat of exhaust flue gas can also be used to drive an organic Rankine cycle to produce electric power [5, 12–14].

The latent heat of the exhaust steam from a condensing turbine is released to the cooling water at the condenser as shown in **Figure 1**. Even for a modern steam turbine, 50–60% of the heat input is discharge to the heat sink. Seawater is generally used as the cooling water for the offshore power plants. The seawater at high-latitude regions or at deep sea (depth down to 1000 m) has a temperature as low as 5°C. However, the condensing turbine exhaust pressures are generally higher than 3.5kPa with condensation temperatures not less than 26.7°C due to the limits from the wetness loss, last-stage blade length, and droplet erosion. Thus, the temperature difference between the exhaust steam and seawater can be used to drive an ORC to produce electricity. An ORC can also use a part of the extracted steam from low-pressure turbine and boiler flue gas [14] or only the coldest extraction steam [15] to generate additional electricity.

In coal-fired power plants, there are different kinds of heat sources which can be utilized by ORCs. The waste heat sources involve different heat transfer fluids (gas, water, and steam) and large scales of capacity and temperature. The exhaust flue gas with temperatures up to 140°C from a supercritical boiler which contains

10–30 MW heat can be recovered. The turbine exhaust steam at 30°C contains more than 300 MW heat for a large-capacity power unit. Therefore, this chapter focuses on the thermodynamic performance of ORCs using the waste heat from coal-fired power plants. The suitable cycle layouts are discussed with considering the waste heat source characteristics. The evaporation temperature and pressure of the working fluid will be optimized to maximize the cycle net power output. The proper working fluid is selected according to the thermodynamic performance. The power generation potentials are also evaluated for various kinds of waste heat sources.

2. ORC model

The ORCs using low-boiling organic working fluids are the unequaled technology for producing electricity from medium-low-temperature heat sources [16]. The ORCs have distinctive features of being simple layouts, being efficient for off-design conditions, and being reasonable cost-effectiveness. Therefore, ORC systems have been widely used to convert geothermal, solar, biomass, waste heat, and ocean thermal energy to electricity. The theoretical basis for ORCs has been described elsewhere [16–22]. This section briefly describes the cycle layouts and working fluids selection.

2.1 Cycle layouts

The ORCs can be classified into subcritical and supercritical cycles according to the working fluid evaporation pressure. Considering the saturated vapor line shapes of working fluids, the subcritical ORC with saturated vapor at the turbine inlet is called o2 cycle, and that with superheated vapor at the turbine inlet is called o3 cycle which uses a dry working fluid or b3 cycle which uses a wet working fluid, and the supercritical ORC is called s2 cycle [17]. The cycle layouts are selected according to the heat source characteristics and the working fluid critical temperature. **Figure 2(a)** shows a typical ORC system with a wet cooling system with the *T-s* diagrams for o2, o3, b3, and s2 cycles shown in **Figure 3**. The working fluid is heated to a saturated or a superheated vapor from a subcooled liquid by the heat source fluid in heat exchangers. Thus, the energy balance for working fluid evaporation can be uniformly expressed as

$$\dot{m}_{\mathrm{H}}(h_{\mathrm{Hin}} - h_{\mathrm{Hout}}) = \dot{m}_{\mathrm{O}}(h_0 - h_3) \tag{1}$$

where h is the specific enthalpy, the subscript H represents the heat source, and the subscript O represents the organic fluid.

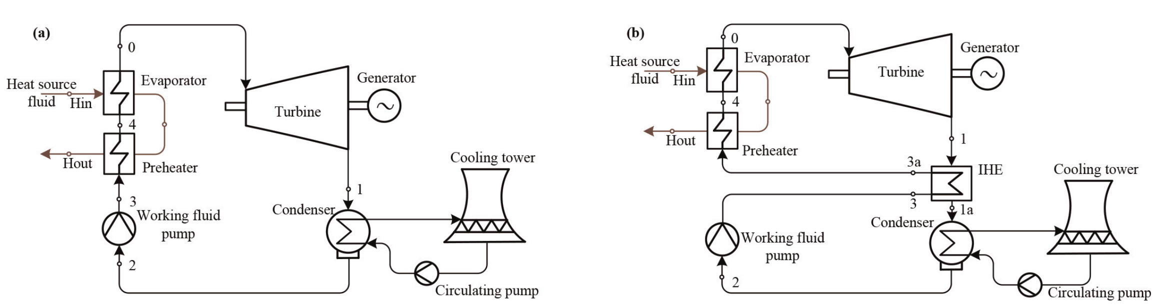

Figure 2.
Schematics of (a) a typical ORC and (b) an ORC with an IHE.

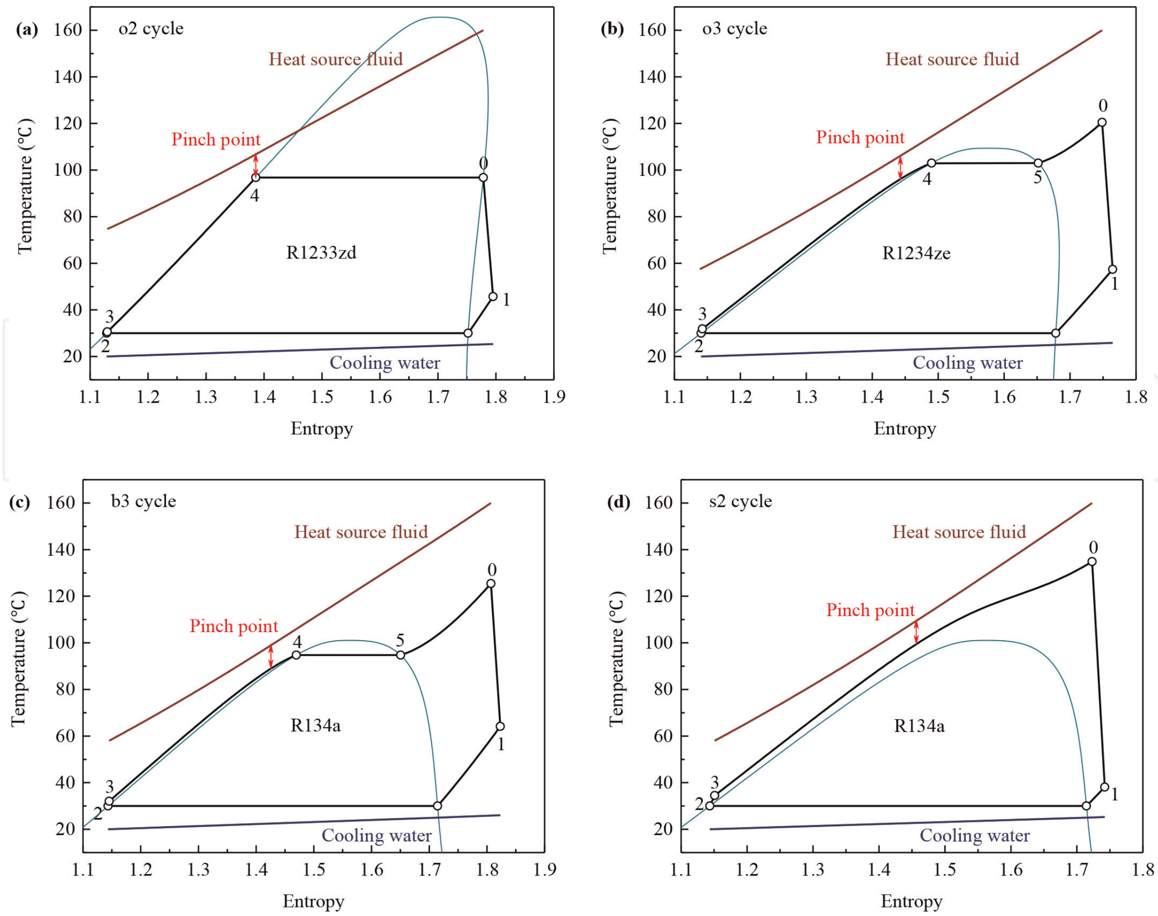

Figure 3.
Temperature-entropy diagrams for basic ORCs: (a) o2 cycle, (b) o3 cycle, (c) b3 cycle, and (d) s2 cycle.

The power generated by the turbine was

$$\dot{W}_{\mathrm{T}} = \dot{m}_{\mathrm{O}}(h_0 - h_1) \tag{2}$$

The power consumed by the working fluid feed pump was

$$\dot{W}_{\mathrm{FP}} = \dot{m}_{\mathrm{O}}(h_3 - h_2) \tag{3}$$

The net power output by the ORC system was defined as the turbine power output which subtracts the parasitic power consumed by the working fluid feed pump:

$$\dot{W}_{\mathrm{net}} = \dot{W}_{\mathrm{T}}\eta_{\mathrm{m}}\eta_{\mathrm{g}} - \dot{W}_{\mathrm{FP}} \tag{4}$$

The cycle thermal efficiency is defined as

$$\eta_{\mathrm{th}} = \frac{\dot{W}_{\mathrm{net}}}{\dot{Q}_{\mathrm{in}}} \tag{5}$$

The turbine exhaust vapor temperature could still be relative high; the superheated vapor could be worth preheating the working fluid in an internal heat exchanger (IHE), also referred to as a recuperator or regenerator, before the preheater [16–18] as shown in **Figure 2(b)**. Eq. (1) for an ORC with an IHE can be rewritten as

$$\dot{m}_{\mathrm{H}}(h_{\mathrm{Hin}} - h_{\mathrm{Hout}}) = \dot{m}_{\mathrm{O}}(h_0 - h_{3\mathrm{a}}) \tag{6}$$

The use of an IHE can improve the preheater inlet temperature by the turbine exhaust vapor. For the heat source without the limitation of the outlet temperature [18, 23], the heat source fluid outlet temperature increases because the working fluid is preheated as shown in **Figure 4(a)** and the cycle net power output will maintain constant or increase slightly [24]. For the heat source with a limited outlet temperature as shown in **Figure 4(b)**, the increase in the preheater inlet temperature results in an increase in the working fluid mass flow rate or the optimal evaporation temperature; thus, the net power output increases.

2.2 Systematic parameters

The matching characteristics between the heat source fluid and the working fluid affect the ORC net power output. In subsequent sections, the working fluid evaporation temperature or pressure will be optimized to maximize the cycle net power output. The operating parameters and boundary conditions for the ORCs are listed in **Table 1**. The parametric optimization and thermodynamic analyses are based on the parameters listed in **Table 1** except the ORC in Section 5.2. The heat losses and pressure drops are neglected except instructions.

The pinch point temperature difference is an important parameter for system design and optimization [25, 26]. During the working fluid evaporation, the pinch point may locate at the bubble point, a subcooled liquid state near the critical point and a superheated state [26] which depends on the heat source temperature drop

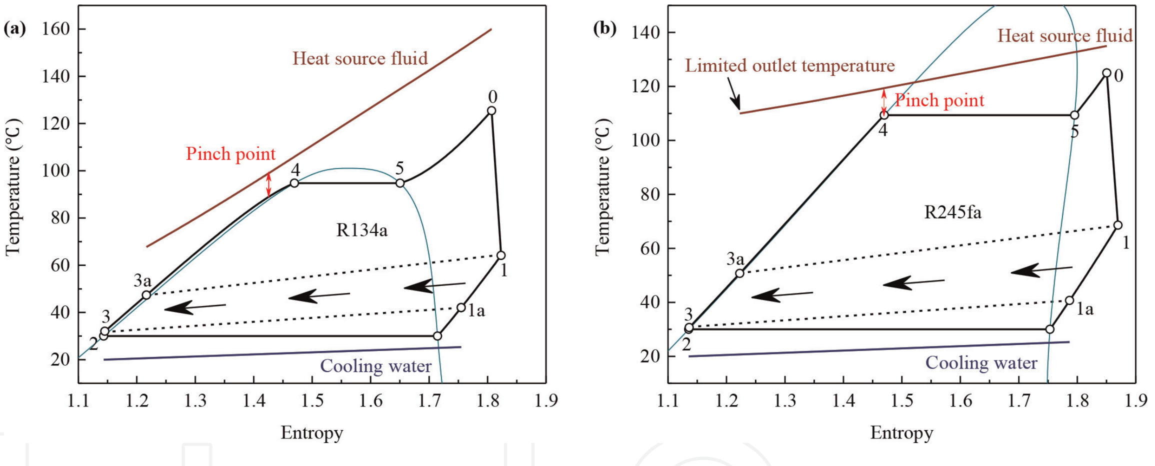

Figure 4.
Temperature-entropy diagrams of ORCs with an IHE for heat source fluids: (a) without outlet temperature limitation and (b) with limited outlet temperature.

Parameters	Values	Unit
ORC turbine isentropic efficiency	85	%
Working fluid pump efficiency	80	%
Generator efficiency	98	%
Turbine mechanical efficiency	98	%
Evaporator pinch point temperature difference	10	°C
IHE pinch point temperature difference	10	°C
Condenser pinch point temperature difference	5	°C
Condensation temperature	30	°C

Table 1.
Parameters and boundary conditions for the ORC systems.

Working fluid	T_{cr}/°C	p_{cr}/MPa	Safety class	ODP	GWP
R134a	101.06	4.059	A1	0	1430
R1234ze(E)	109.36	3.635	A2L	0	6
R236ea	139.29	3.420	n.a	0	1410
R245fa	154.01	3.651	B1	0	1030
R1233zd(E)	165.60	3.572	A1	0.003	1
R123	183.68	3.662	B1	0.01	77

Table 2.
Physical and environmental properties of the six working fluids [29].

and heat capacity and the working fluid thermophysical properties. Thus, each heat exchanger is divided into 100 sections with equal heat-flow interval [25, 27] for determining the pinch point during the parameter optimization.

2.3 Working fluids

Considering the operating safety, nonflammable working fluids are selected for the ORCs using the waste heat in coal-fired power plants. Moreover, the working fluids should be environmentally friendly with a lower ozone depletion potential (ODP) and global working potential (GWP). The critical temperature has been regarded as a criterion for working fluid selection [17, 28]; thus, the studied fluids should cover a wide range of critical temperatures. The selected working fluids here are R134a (1,1,1,2-tetrafluoroethane), R1234ze (1,3,3,3-tetrafluoropropene), R236ea (1,1,1,2,3,3-hexafluoropropane), R245fa (1,1,1,3,3-pentafluoropropane), R1233zd (trans-1-chloro-3,3,3-trifluoropropene), and R123 (2,2-dichloro-1,1,1-trifluoroethane). The physical and environmental properties of the selected working fluids are listed in **Table 2**. The thermophysical properties for the working fluids were calculated using REFPROP 9.1 [29].

3. Waste heat recovery from a boiler blowdown system

3.1 System description

A continuous blowdown system is generally used to purify the steam to maintain acceptable levels of total dissolved solids for a subcritical drum boiler. Part of the saturated boiler water at a higher salt concentration is discharge from the drum to the flash tank [3, 30]. The pressure decreases as the saturated boiler water enters the flash tank. The excess energy in the boiler water is given up as some of the saturated water flashes to the saturated steam. The steam then enters into the deaerator to preheat the boiler feedwater, and the drain is generally discharge to the sewer. The energy in the drained liquid is lost through direct discharge.

The drain temperature is generally higher than 150°C. Here, an organic Rankine cycle (ORC) is designed to recover the waste heat of the drained water from a continuous blowdown system for power generation and then to improve the overall thermal efficiency of the power plant [4]. The organic working fluid is heated by the waste heat in the discharged drain and then generates power by expansion through a turbine as shown in **Figure 5**.

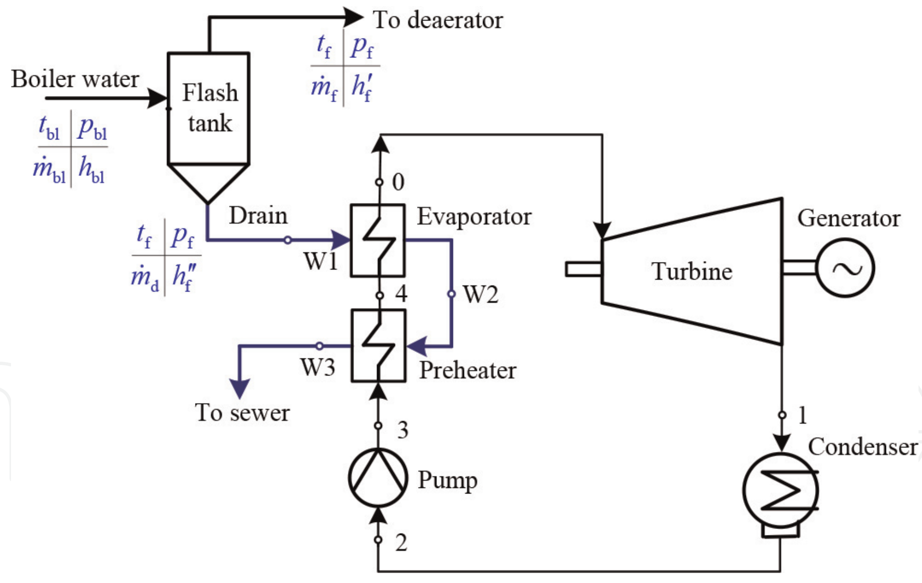

Figure 5.
Schematic of an ORC power generation system using the blowdown waste heat from a subcritical boiler [4].

The energy balance for the flash tank can be expressed as

$$\dot{m}_{\mathrm{bl}} h_{\mathrm{bl}} \eta_{\mathrm{f}} = \dot{m}_{\mathrm{f}} h_{\mathrm{f}}'' + \dot{m}_{\mathrm{d}} h_{\mathrm{f}}' \tag{7}$$

where $\dot{m}_{\mathrm{bl}}$ is the boiler water flow rate, h_{bl} is the specific enthalpy of the boiler water, η_{f} is the flash tank efficiency which is set to be 0.98, $\dot{m}_{\mathrm{f}}$ is the saturated steam flow rate, $\dot{m}_{\mathrm{d}}$ is the drained water flow rate, h_{f}'' is the specific enthalpy of the saturated steam, and h_{f}' is the specific enthalpy of the drained water.

The mass balance for the flash tank can be expressed as

$$\dot{m}_{\mathrm{bl}} = \dot{m}_{\mathrm{f}} + \dot{m}_{\mathrm{d}} \tag{8}$$

The flow rate of the saturated steam flashed from the boiler water increases as the flash tank pressure, p_{f}, decreases. The flash tank pressure generally is set to be the deaerator pressure which ranges from 0.8 to 1.1 MPa for subcritical steam turbines. Thus, 40–50% of the boiler water is flashed into saturated steam.

The main-steam flow rates of typical subcritical 600 MW power units range from 1600 to 2000 t/h for the BRL (boiler rated load) condition. About 13–16 t/h boiler water enters the flash tank if the blowdown rate is 0.8% which means that the drained water flow rate can reach 6–10 t/h. A power plant generally has 2–8 power units; thus, the drain water from the continuous blown down systems can be collected, and the flow rate may be reached 80 t/h.

A typical subcritical 600 MW boiler is analyzed in this section. The boiler parameters for the BRL condition are listed in **Table 3**. The boiler water flow rate in a blowdown system is set to be 17.1 t/h. At the flash tank outlet, the drain flow rate is 9 t/h according to Eqs. (7) and (8). Assume a power plant has same four power units; thus, the total drain flow rate is 10 kg/s (36 t/h). The collected drain is used to drive an ORC as shown in **Figure 5**. Considering the heat loss, the drain temperature to the ORC system is set to be 180°C.

3.2 Thermodynamic performance

The turbine inlet temperatures (pressure) were optimized to maximize the cycle net power output for the ORCs with saturated vapor at the turbine inlet (o2 cycle)

Parameters	Values	Unit
Main-steam flow rate	2011	t/h
Steam drum pressure	18.5	MPa
Boiler water temperature in drum	359.3	°C
Flash tank pressure	1.03	MPa
Drain temperature	181.2	°C
Flash tank efficiency	98	%
Drain flow rate	10	kg/s
Drain pressure	1.03	MPa
Drain temperature at the evaporator inlet	180	°C

Table 3.
Blowdown system parameters of a 600 MW boiler for the BRL condition.

Working fluid	Cycle	$T_{T,in}$/°C	$P_{T,in}$/MPa	Power output/kW	Heat utilization ratio/%
R245fa	o2	116.3	1.79	660	70.99
R1233zd(E)	o2	109.8	1.28	622	68.08
R123	o2	106.4	0.90	599	65.88
R134a	b1	169.6	3.06	548	75.81
R1234ze	o3	153.0	2.63	567	76.47
R236ea	o3	121.4	2.06	677	77.81
R134a	S2	163.4	8.57	749	77.10
R1234ze	S2	163.7	7.48	746	77.10
R236ea	S2	160.7	4.95	764	77.10

Table 4.
Parameters of the ORC for waste heat recovery from a blowdown system.

using R245fa, R1233zd(E), and R123. The optimized turbine inlet temperatures and the maximum net cycle power outputs are listed in **Table 4**. The results show that the optimal turbine inlet temperature decreases as the critical temperature of the working fluid increases. The net power output as well as the waste heat utilization rate decreases for working fluids with higher critical temperatures. The net cycle power output is 660 kW for the o2 cycle using R245fa, while the net cycle power output is only 599 kW for the o2 cycle with R123.

Here, the superheated ORC uses a working fluid with a lower critical temperature (R134a, R1234ze, and R236ea) for recovering the waste heat from the drained water. The turbine inlet temperature and pressure are optimized simultaneously to obtain the maximum cycle net power output using the generalized reduced gradient (GRG) method which has been successfully used in previous work [4, 27]. Both the optimized turbine inlet temperature and pressure are higher for the working fluid with lower critical temperature as shown in **Table 4**. However, the working fluid with higher critical temperature generates a higher net power due to the higher working fluid flow rate. The net cycle power output with R236ea is higher than that with R134a or R1234ze.

A supercritical ORC provides a better match between the working fluid and the heat source fluid temperature profiles. The working fluids with much lower critical temperatures, such as R134a, R1234ze, and R236ea, are considered here for supercritical ORCs. The turbine inlet temperature and pressure are optimized simultaneously to maximize the cycle net power output considering the pinch point temperature difference limit. Compared with subcritical ORCs, a supercritical ORC produces 13–37% more net cycle power as shown in **Table 4**. The optimal turbine inlet temperatures for supercritical ORCs with the selected working fluids are very close; however, the working fluid with a lower critical temperature has a higher optimal turbine inlet pressure. The high operating pressure and heat transfer deterioration due to the large specific heat near the critical point must be considered in the system design [4]. The supercritical ORC using R236ea generates the highest net power (764 kW) among the considered ORCs with the selected working fluids.

4. Waste heat recovery from boiler exhaust flue gas

The heat loss in the exhaust flue gas is the largest heat loss in a power station boiler which typically accounts 70–80% of the total boiler heat losses [30]. The temperature of the exhaust flue gas from a power station boiler generally ranges from 120–140°C. Unfortunately, the flue gas temperature may be higher than the design value in operation which results in more heat losses and lower boiler thermal efficiencies. The exhaust flue gas can be cooled by a low-boiling organic working fluid with the fluid then passing through a turbine to generate power. The potential decrease in the exhaust flue gas temperature is 10–30°C. Supercritical 1000 MW boilers for power plants consume about 350 tons of bituminous coal and generate about 3×10^6 Nm^3 flue gas per hour for the BRL condition. More than 10 MW waste heat can be recovered to drive an ORC when the flue gas temperature is reduced by 10°C. This section discusses the thermodynamic performance of ORCs using the flue gas waste heat from a supercritical boiler.

4.1 Coal-fired boiler

More than 90 supercritical 1000 MW coal-fired power units are being operated in China with more 1000 MW power units planned to replace many current small-capacity and low-efficiency power units [31]. Therefore, a modern supercritical 1000 MW power unit is taken here as a case study. The boiler operating parameters for the BRL condition are listed in **Table 5**. The main-steam temperature is 605°C with a flow rate of 800.5kg/s. The exhaust steam from the high-pressure steam turbine is then reheated to 603°C in the reheater with a flow rate of 649kg/s. The feedwater temperature at the economizer inlet is 299.4°C with no water and steam assumed to be lost in the boiler. The exhaust flue gas temperature is 135°C, and the boiler thermal efficiency is 92.57%.

The ultimate analysis (UA) of the fuel is useful for the calculation of air and flue gas quantities and other combustion calculations [3, 30]. The coal consists of five elements (carbon, hydrogen, nitrogen, oxygen, and sulfur), moisture, and ash. A typical bituminous coal is used here as the boiler fuel. The elemental weights of the coal are determined on as-received basis: C_{ar} = 61.7%, H_{ar} = 3.67%, O_{ar} = 8.56%, N_{ar} = 1.12%, S_{ar} = 0.6%, A_{ar} = 8.8%, and M_{ar} = 15.55%. The lower calorific value (LCV) of the bituminous coal is 23.47 MJ/kg. The boiler consumes 353.5 tons of bituminous coal and generates 3.055×10^6 Nm^3 flue gas per hour for the BRL condition.

Sulfur in the coal on combustion forms SO_2 and partly SO_3. Sulfuric acid will be formed because of the reaction between SO_3 and H_2O in the flue gas at lower temperatures, which then condenses on the tube surface below the acid dew point and leads to the corrosion of the tubes [3, 30]. Therefore, the flue gas was assumed to be cooled to 110°C by the organic working fluids to avoid low-temperature corrosion.

Parameters	Values	Unit
Main-steam temperature at superheater outlet	605	°C
Main-steam pressure at superheater outlet	26.13	MPa
Main-steam flow rate	800.49	kg/s
Steam temperature at reheater outlet	603	°C
Reheated steam pressure at reheater outlet	4.57	MPa
Steam temperature at reheater inlet	347.7	°C
Reheated steam pressure at reheater inlet	4.80	MPa
Reheated steam flow rate	648.96	kg/s
Feedwater temperature	299.4	°C
Boiler thermal efficiency	92.57	%
Exhaust flue gas temperature	135	°C
Lower calorific value (LCV) of coal	23469.7	kJ/kg

Table 5.
Operating parameters of a supercritical 1000 MW boiler for the BRL condition.

4.2 ORC system driven by waste heat from boiler flue gas

Figure 6 shows an ORC system using waste heat of flue gas from a boiler for power generation. A counterflow heat exchanger is used here to recover the waste heat because the flue gas temperature is much lower. The heat exchanger tubes are placed in an in-line arrangement for a lower flue gas pressure drop. The flue gas longitudinal flows outside the tubes. The working fluid is heated to a vapor from a subcooled liquid in the tubes of the heat exchanger.

The heat source temperature is a key parameter which influences the choice of cycle types and working fluids [16–19, 23]. The flue gas temperature should be higher than the acidic dew point to avoid low-temperature external corrosion; thus, the temperature drop of the exhaust flue gas from power station boiler is much lower. Considering the lower temperature drop and the higher flue gas temperature at the preheater outlet, an internal heat exchanger (IHE) is used in the ORC system to improve the working fluid temperature at the preheater inlet by the turbine exhaust vapor and then decrease the temperature difference between the flue gas and the working fluid.

The energy balance in the heat exchanger can be expressed as

$$\dot{B}V_{\text{fg}}\left(I_{\text{fg}}^{\text{in}} - I_{\text{fg}}^{\text{out}}\right)\eta_{\text{HE}} = \dot{m}_{\text{O}}(h_0 - h_{3\text{a}}) \tag{9}$$

where $\dot{B}$ is the coal consumption rate, V_{fg} is the specific volume flue gas based on 1 kg coal (unit flue gas volume), $I_{\text{fg}}^{\text{in}}$ is the flue gas enthalpy at the heat exchanger inlet, and $I_{\text{fg}}^{\text{out}}$ is the flue gas enthalpy at the heat exchanger outlet, η_{HE} is the heat exchanger efficiency which considering the heat loss, $\dot{m}_{\text{o}}$ is the organic working fluid flow rate, h_0 is the working fluid specific enthalpy at the heat exchanger outlet, and $h_{3\text{a}}$ is the specific enthalpy at the IHE outlet.

The unit gas weights (volumes) for the BRL condition were calculated using the ultimate analysis [3, 30]. The excess air coefficient in the flue gas was assumed to be 1.3. The heat-flow rate is 29.26 MW when the flue gas temperature is reduced from 135 to 110°C. The total heat loss is assumed to be 5% during the heat transfer due to the radiation and convection; thus, 27.8 MW heat is transferred to the organic

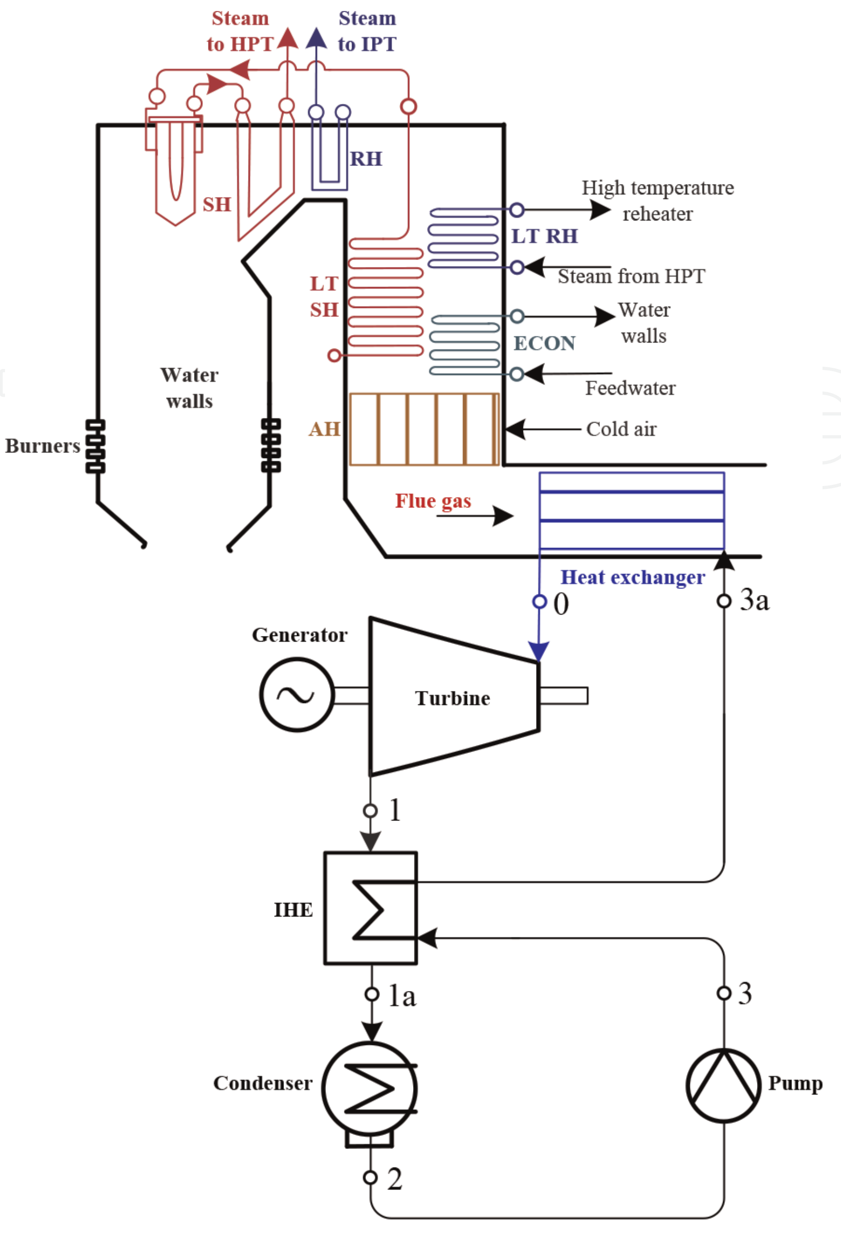

Figure 6.
Schematic of an ORC system using waste heat of flue gas from a boiler.

working fluids. The heat losses and pressure drops in the ORC system are neglected to simplify the calculations.

4.3 Thermodynamic performance

Both the o2 cycle and the o3 cycle are studied with the working fluids of R123, R1233zd, R245fa, and R236ea. The evaporation temperatures (pressures) of the selected working fluids were optimized for the o2 cycle to maximize the net cycle power output. The optimized parameters and system performance are listed in **Table 6**. **Figure 7(a)** shows the T-Q diagrams of the selected working fluids for o2 cycle. The optimal evaporation temperature of the o2 cycle is lower for the working fluid with a higher critical temperature which results in a higher heat load for the isothermal evaporation process and a better match between the working fluid and the flue gas temperatures as shown in **Figure 7(a)**. The working fluid with a higher critical temperature also has a lower evaporation pressure which leads to a lower working fluid pump power consumption. For example, 61.7% of the total heat flow is used for R123 boiling process, while 54.3% of the total heat flow is needed for R236fa preheating which process has a large temperature difference. Therefore, the

Working fluid	Cycle	$T_{T,in}$/°C	$P_{T,in}$/MPa	Power out/kW	Thermal efficiency/%
R236ea	o2	113.67	2.09	3783.0	13.61
R245fa	o2	111.84	1.63	3845.9	13.84
R1233zd(E)	o2	110.69	1.31	3876.9	13.95
R123	o2	109.60	0.97	3937.7	14.17
R134a	b3	125	3.85	3502.0	12.60
R1234ze	o3	125	2.74	3570.6	12.85
R236ea	o3	125	1.97	4025.5	14.48
R245fa	o3	125	1.55	4070.6	14.65
R1233zd(E)	o3	125	1.25	4074.6	14.66
R123	o3	125	0.93	4118.6	14.82
R134a	s2	125	4.26	3484.8	12.54
R1234ze	s2	125	3.82	3576.5	12.87

Table 6.
Comparison of ORCs using flue gas waste heat from a 1000 MW boiler.

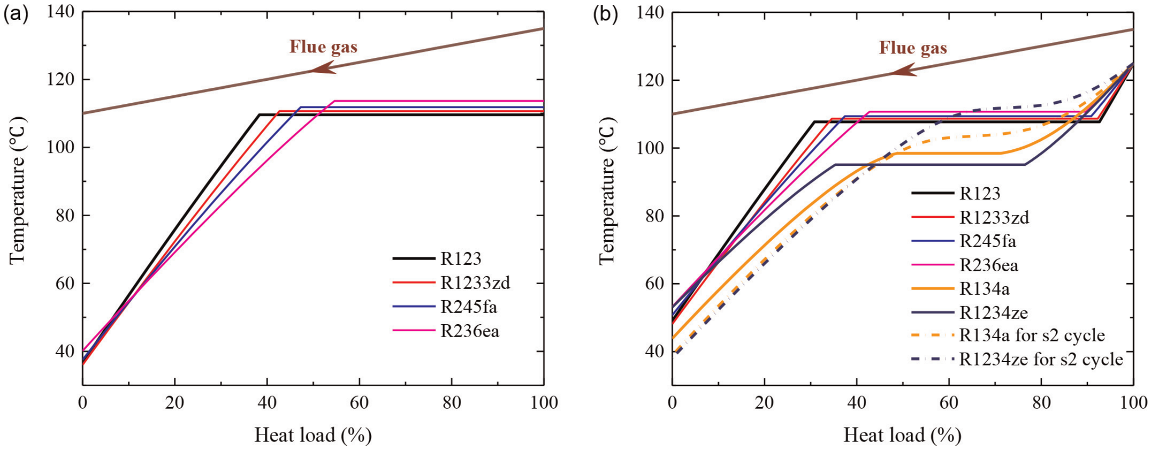

Figure 7.
T-Q diagrams for (a) the o2 cycles and (b) the cycles with superheated vapor or supercritical fluid at the turbine inlet.

o2 cycle using a working fluid with a higher critical temperature produces more net power as shown in **Table 6**. The o2 cycle using R123 generates about 4% more net power than that using R236ea.

Increasing the heat load of the isothermal evaporation process can better match the temperature profiles between the flue gas and the working fluid due to the lower temperature drop of the flue gas. The subcritical cycle using superheating process can further improve the temperature matching between the flue gas and the working fluid. The turbine inlet temperatures of the selected working fluids were set here to be 125°C for the subcritical cycles, and then the evaporation pressures were optimized to obtain the maximum net cycle power with the minimum temperature difference between the flue gas and the working fluid not less than 10°C. Compared to the o2 cycle, the use of superheating results in a slight decrease in the evaporation pressure and then reduces the power consumption of the working fluid pump. The turbine exhaust vapor temperature increases about 18°C due to the superheat degree at the turbine inlet; however, the working fluid temperature in the IHE can be increased by 12–13°C by the waste heat from the turbine exhaust vapor. Therefore, the average heat transfer temperature difference between the flue gas and the working fluid decreases, and the o3 cycle produces more power than the o2 cycle as shown in **Table 6**.

In this case study, the working fluid with a higher critical temperature needs a lower heat load for superheating and a higher heat load for boiling as shown in **Figure 7(b)**. For instance, the heat load for R123 superheating accounts for 7.4%, and the heat load for R123 boiling accounts for 61.8% of the total heat load; however, the heat load for R134a superheating accounts for 28.8%, and the heat load for R134a boiling only accounts for 22.4% of the total heat load because the boiling temperature is close to its critical temperature. The working fluids with lower critical temperatures have higher optimal evaporation pressures which also results in more power consumed by the working fluid pump. The ORC with superheating using R123 as the working fluid can generate 17.6% more power than that using R134a.

The supercritical ORCs using R1234ze and R134a which has a lower critical temperature are analyzed and compared here. The turbine inlet temperature is also set to be 125°C with the turbine inlet pressure of 1.05 p_{cr} because the turbine inlet temperature is very close to the critical temperature. The supercritical ORCs with R134a and R1234ze give a better matching of the temperature profiles between the working fluid and the flue gas compared to the subcritical ORCs as shown in **Figure 7(b)** which results in a higher turbine power output; however, the power consumed by the working fluid pump increases with increasing evaporation pressure which offsets the advantages of the supercritical ORCs. For example, the net power output of the supercritical ORC with R134a is even lower than the subcritical ORC for this case study. The subcritical ORC with superheating (o3 cycle) shows a better thermodynamic performance for lower temperature drop heat sources. The maximum power is produced by o3 cycle with R123 for waste heat recovery from the flue gas at a temperature of 135 °C, followed by o3 cycle with R1233zd and R245fa in this case study.

The volume flow rate at the turbine inlet as well as the turbine outlet/inlet volumetric flow ratio is important for the turbine design [17, 26]. **Figure 8(a)** shows the thermal efficiencies as a function of the turbine inlet volume flow rates of the working fluids for the optimal conditions. The mass flow rates of the selected working fluids are very close which range from 119 to 146 kg/s. However, a lower turbine inlet pressure leads to a lower density; thus, the working fluids evaporated at lower pressures have a much higher volume flow rates. The volume flow rate of R123 is the highest for the o2 cycle among the working fluids. Compared to the o2

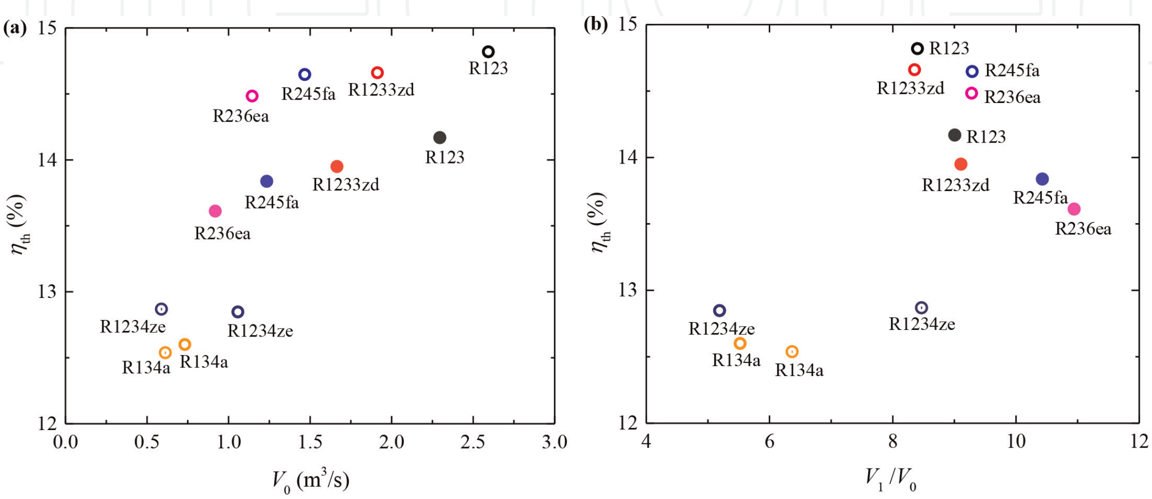

Figure 8.
Thermal efficiencies versus (a) volume flow rate, V_o, at the turbine inlet and (b) turbine outlet/inlet volumetric flow rate ratios for the optimal condition: ● saturated vapor, ○ superheated vapor, and ⊙ supercritical fluid.

cycle, the volume flow rate is increased by 10–20% for the o3 cycle due to the lower turbine inlet pressure as shown in **Figure 8(a)**, while the thermal efficiency can be increased by 4.6–6.4%. Both the R134a and R1234ze have lower volume flow rates with lower thermal efficiencies. The working fluid has a higher volume flow rate at the turbine inlet, also somewhat has a higher thermal efficiency as shown in **Figure 8(a)**.

Figure 8(b) shows the thermal efficiencies as a function of the VR (turbine outlet/inlet volumetric flow rate ratios, V_1/V_0) at the optimum turbine parameters for the maximum power output. Compared to the o2 cycle, the expansion ratio in the turbine decreases for the o3 cycle with the same condensation pressure which also leads to a decrease in the VR. Both the expansion ratios of R134a and R1234ze are much lower in the subcritical ORC because of the higher condensation pressures which also results in lower VRs. The VRs of R134a and R1234ze are increased in the supercritical ORC. Among the selected working fluids, R123, R1233zd, and R245fa have high thermal efficiencies with high-turbine-inlet volume flow rates and turbine outlet/inlet volumetric flow rate ratios. R1233zd is considered to be the most suitable working fluid for the ORC which recovers waste heat from the boiler flue gas with taking the safety and environment protection into account.

5. Heat recovery from turbine exhaust steam

5.1 ORCs driven by exhaust steam from a back-pressure turbine

Back-pressure steam turbines supply not only electricity but also the steam and heat for processes. The exhaust steam of the back-pressure steam turbine is directly used to supply heat or steam to the facilities without condensation. Ideally, the exhaust steam and the electricity from the back-pressure steam turbine are supplied to the same users [32]. The back-pressure steam turbine does not have any cold source loss (heat loss released directly to the environment). Therefore, the back-pressure steam turbines are efficient and have been widely used in industrial applications such as oil refineries, petrochemical plants, and cogeneration [33].

The exhaust steam pressure generally is set to be the demand pressure from the facility or outside needs [33]; thus, a lower expansion ratio results in a lower enthalpy drop and small power output in a back-pressure steam turbine. Only fewer turbine stages are used due to the lower enthalpy drop which leads to a simple structure and a lower cost for a back-pressure steam turbine.

Process steam/heat demand and electricity demand change independently according to the season or facility production demand [33]. An imbalance between process steam/heat and electricity demands is one of the most common problems in actual operation. The steam/heat demand is the primary requirement with electricity demand a secondary consideration to solve the imbalance demands because the steam and heat cannot economically and conveniently be transported over a long distance. Adjusting the main-steam flow rate of a back-pressure turbine is the major solution to meet the steam/heat demand. Thus, the back-pressure turbine power (electricity) output varies with the steam/heat demand. However, the thermal efficiency of the back-pressure steam turbine is significantly decreased with decreasing electricity output at partial loads due to the lower enthalpy drop. For example, the turbine isentropic efficiency (relative internal efficiency) can be decreased from 85 to 60% for lower steam flow rates which leads to an increase in the heat consumption of power generation [34].

The imbalance between steam/heat and electricity demands reduces the economic performance of back-pressure steam turbines. Part of this risk will be mitigated if the back-pressure steam turbine can be operated at the optimum condition (design condition) and the excess steam which beyond the steam/heat demand is used to generate electricity by an ORC which exports electricity directly into the grid [32]. The back-pressure turbine will operate with constant steam flow rate, but the steam flow rate to the ORC system varies with the steam/heat demand. The ORCs have the distinctive features of being simple cycle layouts, being low cost and especially being efficient for partial loads. Therefore, an ORC can generate power using the excess steam with high thermal efficiency and availability for complex operating conditions. In this conceptual system, the back-pressure steam turbine is operating efficiently at the optimal condition, and the extra electricity generated from the ORC system is sold to the grid which improves the economics considerably.

A typical B25–8.83/1.5 extraction back-pressure turbine is taken as a case study. The parameters for typical conditions of the back-pressure turbine are listed in **Table 7**, and the schematic is shown in **Figure 9**. The superheated steam from the boiler enters the back-pressure steam turbine to generate power. One stage steam is extracted from the steam turbine for the feedwater heater 1 (FWH1) to preheat the feedwater. In the original system, the exhaust steam of the back-pressure turbine is divided into four stages of steam flow: one stage extracted from the exhaust steam for FWH2 to preheat the feedwater, one stage extracted for the deaerator after throttling, one stage extracted for the mixer after throttling to a lower pressure to

Parameters	THA	75%THA	50%THA	30%THA
Main-steam temperature/°C	535	535	535	535
Main-steam pressure/MPa	8.83	8.83	8.83	8.83
Main-steam flow rate/$t{\cdot}h^{-1}$	245	195	148	109
Power output/kW	25,203	18,862	12,637	7545
Exhaust steam temperature/°C	316.2	327	345.3	370.6
Exhaust steam pressure/MPa	1.5	1.5	1.5	1.5
Steam demand/$t{\cdot}h^{-1}$	174.5	140.9	108.6	81.0
Isentropic efficiency/%	79.5	74.77	66.77	55.87

Table 7.
Operating parameters for a B25–8.83/1.5 back-pressure turbine [34].

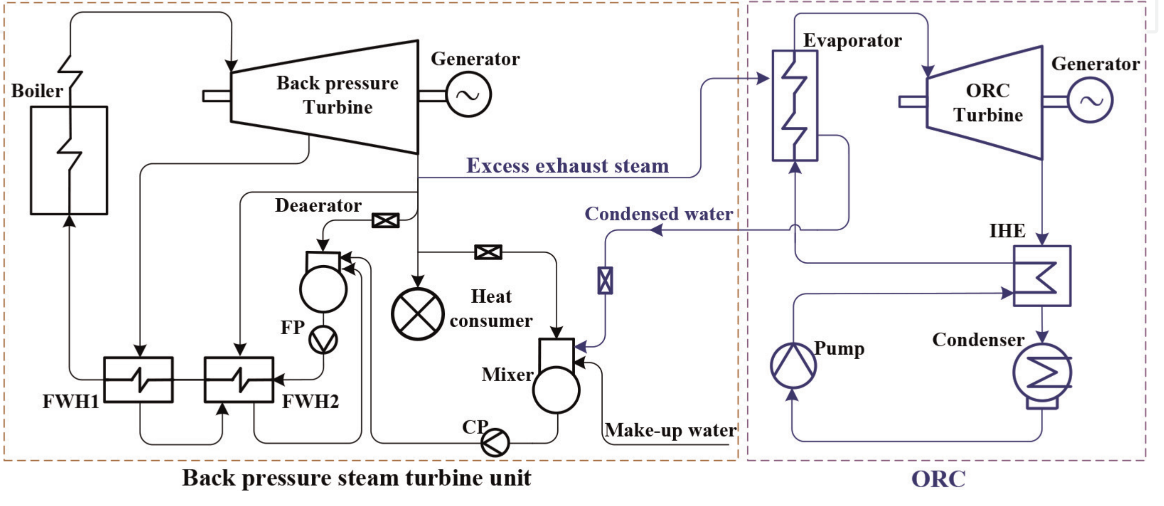

Figure 9.
Schematic of an ORC for recovering the excess exhaust steam heat from a back-pressure steam turbine [34].

preheat the makeup water, and the rest most of exhaust steam transported to the heat consumer. The heat consumer steam demand accounts for 70% of the turbine main-steam flow. The main-steam flow rate of the back-pressure turbine decreases with decreasing steam demand, which results in a serious decrease in the isentropic efficiency (relative internal efficiency) as shown in **Table 7**.

A conceptual system had been proposed to improve the thermodynamic performance of the back-pressure turbine as shown in **Figure 9** [34]. The back-pressure turbine is always operating at the turbine heat acceptance (THA) condition. When the heat consumer steam demand decreases, the excess exhaust steam is provided to an ORC for organic working fluid heating. The steam is condensed to the saturated water and then returns back to the mixer after throttling to preheat makeup water. Compared to the conditions with lower main steam flow rates, the back-pressure turbine generates additional electricity, $\Delta \dot{W}_{\mathrm{T}}$, due to the high isentropic efficiency and a constant steam flow rate. The amount of electricity produced by the ORC system using the excess exhaust steam is defined as $\dot{W}_{\mathrm{O}}$. Thus, the total additional electricity (increase in electricity) from the system can be expressed as

$$\Delta \dot{W}_{\mathrm{Sys}} = \Delta \dot{W}_{\mathrm{T}} + \dot{W}_{\mathrm{O}} \tag{10}$$

The additional electricity can be provided to the facilities or the grid. The steam/heat and electricity demands can then both be regulated by adjusting the main-steam flow rate. The additional electricity from the back-pressure turbine, $\Delta \dot{W}_{\mathrm{T}}$, mainly depends on the turbine operating parameters and the steam demand. The electricity produced from the ORC system, $\dot{W}_{\mathrm{O}}$, depends on the heat input from the excess exhaust steam and the ORC thermal efficiency [34].

The flow rates of the excess exhaust steam for various steam demands are determined according to the mass and the energy balances in the back-pressure turbine system. The steam in the ORC evaporator is condensed to the saturated liquid. The pressure drop between the back-pressure turbine outlet and the ORC evaporator outlet is set to be 5%. The superheat degree of the exhaust steam reaches 120°C, but the sensible heat is much lower than the latent heat. Thus, the matching characteristics between the organic working fluid evaporation and the steam condensation temperatures affect the ORC thermal efficiency.

The ORC turbine inlet temperature was assumed to be 195°C. The ORC turbine inlet pressures of the selected working fluids were optimized to maximize the net cycle power output with the boundary conditions listed in **Table 1**. The parameters and thermal efficiencies of ORCs are listed in **Table 8**. **Figure 10(a)** shows the *T*-*Q* diagrams of the evaporation process for the selected working fluids. Supercritical cycles are adopted for R134a, R1234ze, R236ea, and R245fa due to their lower critical temperatures and higher heat source temperature, while subcritical ORCs

Working fluid	Cycle	$T_{\mathrm{T,in}}$/°C	$p_{\mathrm{T,in}}$/MPa	$p_{\mathrm{T,out}}$/MPa	Thermal efficiency/%
R134a	s2	195	7.15	0.77	18.99
R1234ze	s2	195	6.09	0.58	19.40
R236ea	s2	195	4.37	0.24	20.59
R245fa	s2	195	3.87	0.18	20.93
R1233zd	o3	195	3.23	0.15	20.93
R123	o3	195	2.80	0.11	21.48

Table 8.
Comparison of ORCs using exhaust steam from a back-pressure turbine.

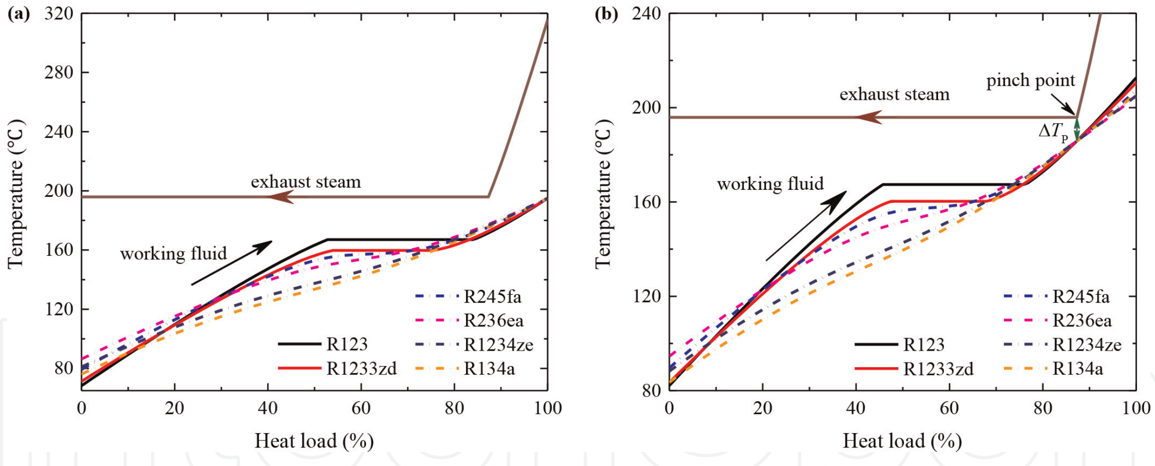

Figure 10.
T-Q diagrams for working fluid evaporating at (a) the optimal pressure and (b) both the optimized pressure and temperature.

with R123 and R1233zd are still used here. Subcritical ORC using R123 with the lowest evaporation pressure shows a better matching of the steam and the working fluid temperature profiles as shown in **Figure 10(a)** and the highest thermal efficiency among the working fluids. The working fluid with a lower critical temperature has a higher evaporation pressure but shows a lower thermal efficiency. The thermal efficiencies for R1233zd and R245fa are very close.

In this conceptual system, the back-pressure turbine outputs 6.3, 12.6, and 17.7 MWh additional electricity for the steam demands of 140.9, 108.6, and 81 t/h, respectively. The additional electricity generation for ORCs using the excess exhaust steam is listed in **Table 9**. As the steam demand decreases to 140.9 t/h, the ORCs generate about 6 MWh electricity with the excess steam flow rate of 44.8 t/h. The ORCs can generate 16.7 MWh electricity when the steam demand is decreased to 81 t/h. Thus, the total additional electricity output of the system, $\Delta\dot{W}_{\text{Sys}}$, can reach 12–34 MWh for partial steam demands.

At last, this section gives a further theoretical discussion on the cycle and working fluid choices for the heat source type with isothermal condensation. Both the temperature and the pressure at the ORC turbine inlet were optimized simultaneously to obtain the maximum power output. **Figure 10(b)** shows the T-Q diagrams for the working fluids evaporating at the optimal condition. The exhaust steam from the back-pressure turbine has a much large superheat degree, but the sensible heat is still much lower than the latent heat. The pinch point occurs at the dew point (saturated vapor state) of the steam as shown in **Figure 10(b)**. The working fluid may be heated to a temperature higher than the steam condensation temperature by the sensible heat. In this case study, the optimal temperatures of the working fluids at the evaporator outlet range from 205–213°C. The working fluid with a higher critical temperature has a higher optimal evaporator outlet temperature and then results in a higher thermal efficiency. The subcritical ORC using the

Steam demand/ $t{\cdot}h^{-1}$	$\dot{W}_O$/kW·h					
	R134a	R1234ze	R236ea	R245fa	R1233zd	R123
140.9	5292	5409	5741	5835	5835	5986
108.6	10,536	10,769	11,429	11,617	11,617	11,918
81.0	14,744	15,069	15,992	16,256	16,256	16,677

Table 9.
Electricity generated by ORCs using excess exhaust steam at various steam demands.

working fluid with a higher critical temperature is more suitable for the kind of isothermal heat source due to the better matches of the temperature profiles of the working fluid and the heat source fluid. The temperature at the evaporator outlet (turbine inlet) strongly affects the cycle thermal efficiency. The cycle efficiency can be relatively increased by about 4% for a 10°C increase in the turbine inlet temperature. Compared to the ORCs with the fixed turbine inlet temperature of 195°C, the cycle efficiencies are relatively improved by 3.7–5.7% for the optimal turbine inlet temperatures and pressures as shown in **Figure 11**. Among the six working fluids, the cycle efficiency with R123 is the highest with the highest turbine inlet temperature, followed by R1233zd. The ORC thermal efficiency can exceed 20% for a steam heat source at a temperature of 200°C. However, the thermal stabilities of the working fluids should be considered primarily [16, 18, 35].

5.2 ORCs driven by exhaust steam form a condensing steam turbine

The majority of heat loss in a steam Rankine cycle is the exhaust steam latent heat released to the coolant at the condenser. The cold source loss generally accounts for 50–60% of the total heat input for an extraction condensing turbine. The steam condensation temperature should be close to the coolant (environment) temperature to reduce the turbine exhaust pressure and then increase the thermal efficiency (absolute internal efficiency). The exhaust pressures generally range 4.9–11.8 kPa for condensing turbines using closed cooling systems with circulating water as the coolant; thus, the exhaust steam is condensed at temperatures of 32.5–49°C with the circulating water flow rate up to 50–100 times the exhaust steam flow rate. The condensation temperature (turbine exhaust pressure) is mainly affected by the environment temperature and the operating conditions. The seawater is generally used as the coolant for offshore power plants. The seawater temperature can reach as low as 5 °C in the cold season or the seawater from a depth up to 1000 m; thus, the turbine exhaust pressures range 3.5–5 kPa with the condensation temperatures between 26.7 and 32.9°C. Considering the issues including wetness fraction, volume flow rate, and blade length of the last stage of the low-pressure turbine (LPT), the exhaust pressure generally does not need to be less than 3.5 kPa even through the cooling water temperature is much lower. The ratio of the

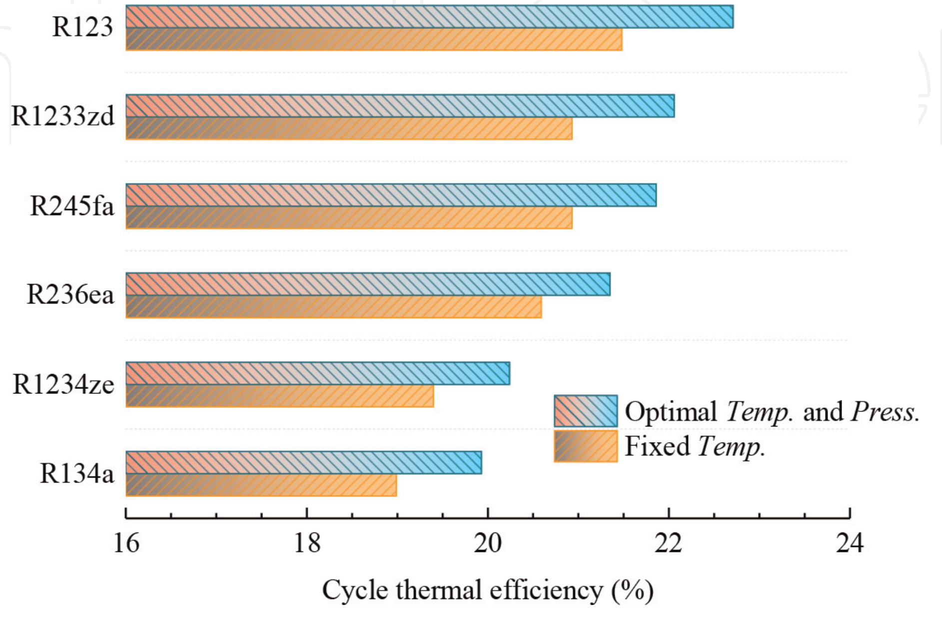

Figure 11.
Cycle thermal efficiencies for the ORCs using exhaust steam from back-pressure turbine.

circulating seawater flow rate to the exhaust steam flow rate can be reduced to 30–50 because of the higher cooling water temperature rise.

Organic Rankine cycles have been studied to utilize the ocean thermal energy with the temperature difference between warm seawater and cold seawater as low as 20°C [36–39]. Therefore, the temperature difference between the turbine exhaust steam and the cooling water can be used to drive an ORC for power generation as shown in **Figure 12**. The exhaust steam from the low-pressure turbine (LPT) is condensed by the organic working fluid in the condenser. The working fluid is heated to a saturated vapor and then enters into the ORC turbine to expand. After expansion, the organic working fluid is condensed by the cold seawater in the ORC condenser. The cycle thermal efficiency of the ORC is lower due to the lower temperature difference between the heat source and sink. However, the ORC can also provide substantial power because the discharged heat from the exhaust steam in a power plant is much huge.

The parameters and boundary conditions for the ORC using exhaust steam as the heat source and cold seawater as the heat sink are listed in **Table 10**. A subcritical 600 MW condensing steam turbine is taken as a case study. The exhaust pressure of the steam turbine is 3.5 kPa with a flow rate of 300 kg/s. The subcritical ORC with saturated vapor at the turbine inlet is only studied here due to the exhaust steam isothermal condensation. The organic working fluid evaporation temperature is only related to the steam condensation temperature with the pinch point temperature difference, ΔT_P; thus, the organic working fluid condensation temperature is the key parameter which affects the thermodynamic performance as shown in **Figure 13**. The ORC thermal efficiency increases as the condensation temperature decreases. A lower condensation temperature needs a lower cooling water (seawater) temperature rise with a higher flow rate; however, the cooling water pumps consume a significant fraction of the ORC output power [27, 36–39]. The cooling water (seawater) flow rate was assumed here to be 45,000 kg/s with a temperature rise about 3.58°C.

Figure 14 shows the turbine power generation and the net power output of the ORC system using the exhaust steam as heat source and the cold seawater as heat sink. The ORC turbine output can exceed 23.5 MW in this case study. The turbine

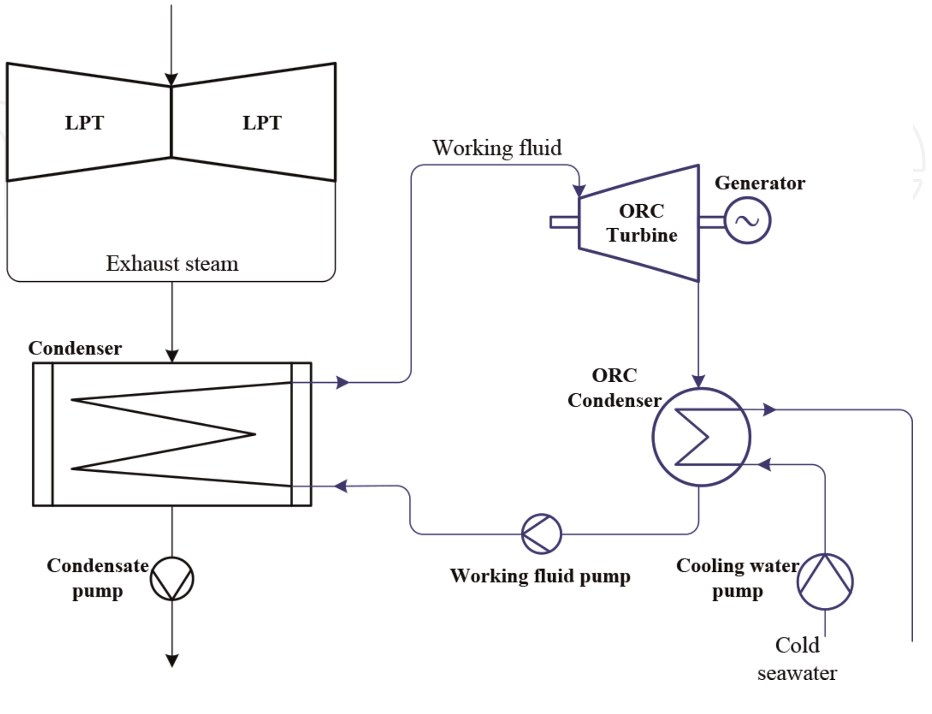

Figure 12.
Schematic of an ORC using the exhaust steam from a condensing turbine and the cold seawater.

Parameters	Values	Unit
Turbine isentropic efficiency [36]	80	%
Working fluid pump efficiency [36]	75	%
Cooling water pump efficiency	80	%
Generator efficiency	98	%
Turbine mechanical efficiency	98	%
Evaporator pinch point temperature difference [37]	2	°C
Condenser pinch point temperature difference	2	°C
Exhaust steam temperature	26.67	°C
Exhaust steam dryness fraction	92	%
Exhaust steam flow rate	300	kg/s
Cold seawater temperature	5	°C
Cooling water (seawater) flow rate	45,000	kg/s
Cooling water pump head	10	m
Seawater specific heat capacity [37]	4.025	kJ/(kg °C)

Table 10.
Operating parameters and boundary conditions for the ORC using exhaust steam as heat source and seawater as sink.

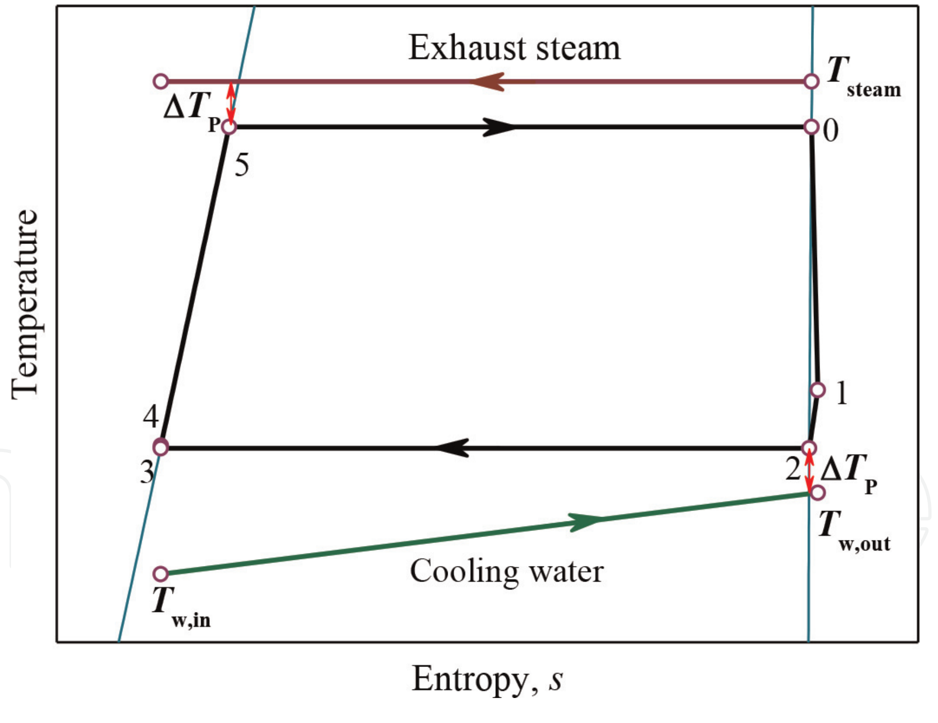

Figure 13.
Temperature-entropy diagram of an ORC using R1234ze as the working fluid driven by exhaust steam from a condensing turbine with cold seawater as heat sink.

using R134a produces the maximum power among the selected six working fluids. The cooling water pumps consume a significant fraction of the turbine output power. The pump power consumption accounts for about 23.3% of the turbine power generation when the cooling water pump head is 10 m. The pressure increase in the working fluid pump is much higher for the working fluid with a lower critical temperature and leads to a higher power consumption. The parasitic power consumed by the working fluid feed pump with R134a accounts for 3.6% of the turbine

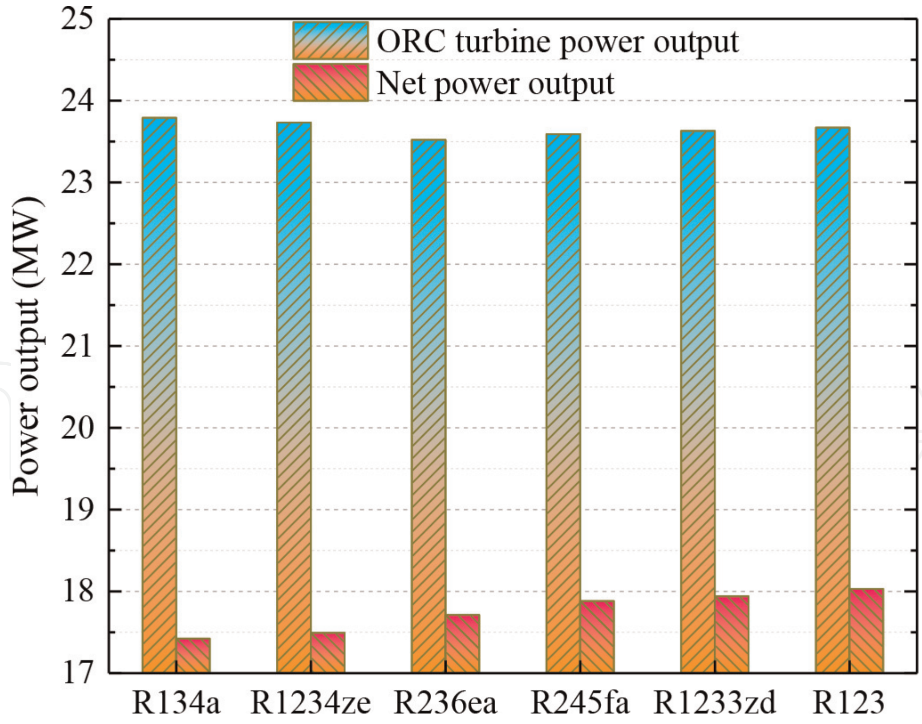

Figure 14.
Turbine power output and net cycle power output for ORCs with exhaust steam as heat source and cold seawater as heat sink.

power output. Thus, the system net power output (subtracting the power consumed by the working fluid pump and the cooling water pumps from the turbine power output) with R134a is the lowest due to the largest parasitic power consumption, while the ORC with R123 outputs the maximum net power among the six working fluids. When the cold seawater is directly used to condense the exhaust steam from LPTs, the cooling water flow rate for the steam turbine is about 8,500 kg/s, but the power consumed by the circulating water pumps is still more than 1 MW. When the exhaust steam is used as an ORC heat source with the cold seawater as the heat sink, the system can provide net power output up to 18 MW equal to 3% increase in the gross power of the coal-fired power unit.

6. Conclusions

In coal-fired power plants, there are a large number of medium-low-grade waste heat which is originally discharge to the environment. Conceptual systems and thermodynamic performance for the ORCs recovering waste heat from coal-fired power plants are studied in this chapter. The optimal cycle layouts and proper working fluids for the ORCs are discussed. The conclusions are summarized as follow.

1. The amount of the drained water that directly discharges has been toward fewer and smaller in modern power plants. The original discharge or leaked drain can be collected to drive a small-capacity ORC. A supercritical ORC matches well with the kind of heat source with a large temperature drop.

2. The flue gas flow rate is much high for a large-capacity boiler. The amount of waste heat in exhaust flue gas can be reached 10 MW even through the flue gas is only cooled by 10°C. The subcritical ORC with an IHE (a recuperator or regenerator) using a working fluid with a higher critical temperature is more

suitable for the kind of heat source with a higher limited outlet temperature. The gross power output of the coal-fired power unit can be relatively increased by 0.4% by the ORC using the waste heat from boiler exhaust flue gas.

3. More than 50% of the heat input to the turbine is released in the condenser. When the cooling water temperature is much lower, the use of ORCs to recover the waste heat from the turbine exhaust steam becomes attractive. Although the cooling water pumps consume a significant fraction of the ORC output power, the net efficiencies of ORCs still reach 2.6%. The power output increase potential for the coal-fired power unit can exceed 2–3% when all of the turbine exhaust steam is used to drive ORCs with lower temperature seawater as the heat sink.

Acknowledgements

This work was supported by the National Natural Science Foundation of China (Grant Nos. 51506223 and 51736005) and the National Basic Research Program of China (973 program) (Grant No. 2015CB251502).

Conflict of interest

The authors declare no competing financial interest.

Author details

Qiang Liu
College of Mechanical and Transportation Engineering, China University of Petroleum, Beijing, P.R. China

*Address all correspondence to: qliu@cup.edu.cn

References

[1] Available from: https://www.iea.org/geco/data/ [Accessed: 08 June 2019]

[2] Available from: https://github.com/citation-style-language/styles/blob/master/vancouver-brackets.csl [Accessed: 08 June 2019]

[3] Che DF. Boilers - Theory, Design and Operation. Xi'an: Xi'an Jiaotong University Press; 2008

[4] Liu Q, Duan YY, Wan XC. Power generation system using continuous blowdown waste heat from drum boiler driving an organic Rankine cycle. Proceedings of the CSEE. 2013;**33**(35): 1-7. DOI: 10.13334/j.0258-8013.pcsee.2013.35.006

[5] Yang YP, Xu C, Xu G, Han Y, Fang YX, Zhang DK. A new conceptual cold-end design of boilers for coal-fired power plants with waste heat recovery. Energy Conversion and Management. 2015;**89**:137-146. DOI: 10.1016/j.enconman.2014.09.065

[6] Liu M, Zhang XW, Ma YG, Yan JJ. Thermo-economic analyses on a new conceptual system of waste heat recovery integrated with an S-CO2 cycle for coal-fired power plants. Energy Conversion and Management. 2018;**161**: 243-253. DOI: 10.1016/j.enconman.2018.01.049

[7] Wang CJ, He BS, Yan LB, Pei XH, Chen SN. Thermodynamic analysis of a low-pressure economizer based waste heat recovery system for a coal-fired power plant. Energy. 2014;**65**:80-90. DOI: 10.1016/j.energy.2013.11.084

[8] Łukowicz H, Kochaniewicz A. Analysis of the use of waste heat obtained from coal-fired units in organic Rankine cycles and for brown coal drying. Energy. 2012;**45**:203-212. DOI: 10.1016/j.energy.2012.03.035

[9] Liu M, Zhang XW, Han XQ, Li G, Yan JJ. Using pre-drying technology to improve the exergetic efficiency of bioenergy utilization process with combustion: A case study of a power plant. Applied Thermal Engineering. 2017;**127**:1416-1426. DOI: 10.1016/j.applthermaleng.2017.08.156

[10] Han XQ, Liu M, Wu KL, Chen WX, Xiao F, Yan JJ. Exergy analysis of the flue gas pre-dried lignite-fired power system based on the boiler with open pulverizing system. Energy. 2016;**106**:285-300. DOI: 10.1016/j.energy.2016.03.047

[11] Han XQ, Karellas S, Liu M, Braimakis K, Chen WX, Yan JJ, et al. Integration of organic Rankine cycle with lignite flue gas pre-drying for waste heat and water recovery from dryer exhaust gas: Thermodynamic and economic analysis. Energy Procedia. 2017;**105**:1614-1621. DOI: 10.1016/j.egypro.2017.03.518

[12] Huang SW, Li CZ, Tan TY, Fu P, Wang LG, Yang YP. Comparative evaluation of integrated waste heat utilization systems for coal-fired power plants based on in-depth boiler-turbine integration and organic Rankine cycle. Entropy. 2018;**20**:89. DOI: 10.3390/e20020089

[13] Xi XM, Zhou YY, Guo C, Yang LJ, Du XZ. Characteristics of organic Rankine cycles with zeotropic mixture for heat recovery of exhaust gas of boiler. Energy Procedia. 2015;**75**: 1093-1101. DOI: 10.1016/j.egypro.2015.07.496

[14] Mikielewicz D, Wajs J, Ziółkowski P, Mikielewicz J. Utilisation of waste heat from the power plant by use of the ORC aided with bleed steam and extra source of heat. Energy. 2016; **97**:11-19. DOI: 10.1016/j.energy.2015.12.106

[15] Angelino G, Invernizzi C, Molteni G. The potential role of organic bottoming Rankine cycles in steam power stations. Proceedings of the Institution of Mechanical Engineers, Part A: Journal of Power and Energy. 1999;**213**:75-81. DOI: 10.1243/0957650991537446

[16] Macchi E. Theoretical basis of the organic Rankine cycle. In: Macchi E, Astolfi M, editors. Organic Rankine Cycle (ORC) Power Systems. London: Woodhead Publishing; 2017. pp. 3-24. DOI: 10.1016/B978-0-08-100510-1.00001-6

[17] Saleh B, Koglbauer G, Wendland M, Fischer J. Working fluids for low-temperature organic Rankine cycles. Energy. 2007;**32**:1210-1221. DOI: 10.1016/j.energy.2006.07.001

[18] Invernizzi CM. Closed Power Cycles - Thermodynamic Fundamentals and Applications. London: Springer-Verlag; 2013. DOI: 10.1007/978-1-4471-5140-1

[19] Astolfi M. Technical options for organic Rankine cycle systems. In: Macchi E, Astolfi M, editors. Organic Rankine Cycle (ORC) Power Systems. London: Woodhead Publishing; 2017. pp. 67-89. DOI: 10.1016/B978-0-08-100510-1.00003-X

[20] Madhawa Hettiarachchi HD, Golubovic M, Worek WM, Ikegami Y. Optimum design criteria for an organic Rankine cycle using low-temperature geothermal heat sources. Energy. 2007;**32**:1698-1706. DOI: 10.1016/j.energy.2007.01.005

[21] Maraver D, Royo J, Lemort V, Quoilin S. Systematic optimization of subcritical and transcritical organic Rankine cycles (ORCs) constrained by technical parameters in multiple applications. Applied Energy. 2014;**117**:11-29. DOI: 10.1016/j.apenergy.2013.11.076

[22] Quoilin S, Broek MVD, Declaye S, Dewallef P, Lemort V. Techno-economic survey of organic Rankine cycle (ORC) systems. Renewable and Sustainable Energy Review. 2013;**22**:168-186. DOI: 10.1016/j.rser.2013.01.028

[23] Zhai HX, An QS, Shi L, Lemort V, Quoilin S. Categorization and analysis of heat sources for organic Rankine cycle systems. Renewable and Sustainable Energy Review. 2016;**64**:790-805. DOI: 10.1016/j.rser.2016.06.076

[24] Sun J, Liu Q, Duan YY. Effects of evaporator pinch point temperature difference on thermo-economic performance of geothermal organic Rankine cycle systems. Geothermics. 2018;**75**:249-258. DOI: 10.1016/j.geothermics.2018.06.001

[25] Pan LS, Shi WX. Investigation on the pinch point position in heat exchangers. Journal of Thermal Science. 2016;**25**:258-265. DOI: 10.1007/s11630-016-0858-7

[26] Liu Q, Duan YY, Yang Z. Performance analyses of geothermal organic Rankine cycles with selected hydrocarbon working fluids. Energy. 2013;**63**:123-132. DOI: 10.1016/j.energy.2013.10.035

[27] Liu Q, Shen AJ, Duan YY. Parametric optimization and performance analyses of geothermal organic Rankine cycles using R600a/R601a mixtures as working fluids. Applied Energy. 2015;**148**:410-420. DOI: 10.1016/j.apenergy.2015.03.093

[28] Xu JL, Yu C. Critical temperature criterion for selection of working fluids for subcritical pressure organic Rankine cycles. Energy. 2014;**74**:719-733. DOI: 10.1016/j.energy.2014.07.038

[29] Lemmon EW, Huber ML, McLinden MO. NIST Standard Reference Database 23: Reference Fluid

Thermodynamic and Transport Properties-REFPROP, Version 9.1. Gaithersburg: National Institute of Standards and Technology, Standard Reference Data Program; 2013

[30] Rayaprolu K. Boilers for Power and Process. Boca Raton: Taylor & Francis Group; 2009

[31] Liu Q, Shang LL, Duan YY. Performance analyses of a hybrid geothermal–fossil power generation system using low-enthalpy geothermal resources. Applied Energy. 2016;**162**: 149-162. DOI: 10.1016/j.apenergy.2015.10.078

[32] Breeze P. Combined Heat and Power. London: Elsevier; 2018. DOI: B978-0-12-812908-1.00003-1

[33] Ohji A, Haraguchi M. Steam turbine cycles and cycle design optimization: The Rankine cycle, thermal power cycles, and IGCC power plants. In: Tanuma T, editor. Advances in Steam Turbines for Modern Power Plants. London: Woodhead Publishing; 2017. pp. 11-40. DOI: 10.1016/B978-0-08-100314-5.00002-6

[34] Liu Q, Duan YY. Cogeneration system coupled with a back pressure steam turbine unit and an organic Rankine cycle (ORC). Proceedings of the CSEE. 2013;**33**(23):29-35. DOI: 10.13334/j.0258-8013.pcsee.2013.23.014

[35] Dai XY, Shi L, Qian WZ. Review of the working fluid thermal stability for organic Rankine cycles. Journal of Thermal Science. 2019;**28**:597-607. DOI: 10.1007/s11630-019-1119-3

[36] Yamada N, Hoshi A, Ikegami Y. Performance simulation of solar-boosted ocean thermal energy conversion plant. Renewable Energy. 2009;**34**:1752-1758. DOI: 10.1016/j.renene.2008.12.028

[37] Aydin H, Lee HS, Kim HJ, Shin SK, Park K. Off-design performance analysis of a closed-cycle ocean thermal energy conversion system with solar thermal preheating and superheating. Renewable Energy. 2014;**72**:154-163. DOI: 10.1016/j.renene.2014.07.001

[38] Khan N, Kalair A, Abas N, Haider A. Review of ocean tidal, wave and thermal energy technologies. Renewable and Sustainable Energy Review. 2017;**72**: 590-604. DOI: 10.1016/j.rser.2017.01.079

[39] Bernardoni C, Binotti M, Giostri A. Techno-economic analysis of closed OTEC cycles for power generation. Renewable Energy. 2019;**132**:1018-1033. DOI: 10.1016/j.renene.2018.08.007